Scalable Mixed-Integer Optimization with Neural Constraints via Dual Decomposition

Shuli Zeng*, Sijia Zhang*, Feng Wu*, Shaojie Tang[†], Xiangyang Li*

*University of Science and Technology of China, Hefei, China
zengshuli0130@mail.ustc.edu.cn, sxzsj@mail.ustc.edu.cn,
wufeng02@ustc.edu.cn, xiangyangli@ustc.edu.cn

[†]State University of New York at Buffalo, Buffalo, NY, USA
shaojiet@buffalo.edu

Abstract—Embedding deep neural networks (NNs) into mixedinteger programs (MIPs) is attractive for decision making with learned constraints, yet state-of-the-art "monolithic" linearisations blow up in size and quickly become intractable. In this paper, we introduce a novel dual-decomposition framework that relaxes the single coupling equality u = x with an augmented Lagrange multiplier and splits the problem into a vanilla MIP and a constrained NN block. Each part is tackled by the solver that suits it best-branch & cut for the MIP subproblem, firstorder optimisation for the NN subproblem—so the model remains modular, the number of integer variables never grows with network depth, and the per-iteration cost scales only linearly with the NN size. On the public SURROGATELIB benchmark, our method proves scalable, modular, and adaptable: it runs $120\times$ faster than an exact Big-M formulation on the largest test case; the NN sub-solver can be swapped from a log-barrier interior step to a projected-gradient routine with no code changes and identical objective value; and swapping the MLP for an LSTM backbone still completes the full optimisation in 47s without any bespoke adaptation.

I. INTRODUCTION

Intelligent decision systems increasingly integrate neural networks into decision-making and optimization pipelines [1–3]. Neural networks provide data—driven surrogates that capture complex, nonlinear dependencies, and their outputs can be enforced as constraints inside mixed-integer programming (MIP) models while preserving the latter's combinatorial guarantees (Fig. 1). This fusion marries the predictive accuracy of data-driven models with the exactness of discrete optimisation: the NN supplies rich, sample-efficient knowledge of latent physics or economics [4–6], while the MIP layer delivers globally optimal and certifiably feasible decisions. As a result, practitioners can exploit learned structure without sacrificing safety guarantees or the ability to produce worst-case certificates—an advantage unattainable by black-box heuristics [7] alone.

Prior research [8–11] has taken important steps toward incorporating neural networks as mathematical constraints. One line of work focuses on **exact, monolithic integration**:

Corresponding authors: Sijia Zhang, Feng Wu, and Xiangyang Li. **Authors' extended version.** Accepted to AAAI-26 (Main Technical Track, Oral). Please cite the conference version. Full appendices and additional experiments are included here.

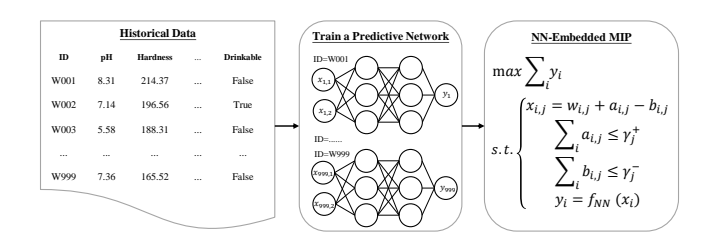


Fig. 1. Workflow of the **NN-Embedded MIP**: historical samples are adjusted under budget constraints, evaluated by a neural classifier, and optimised via a mixed-integer solver.

encoding the network's operations (e.g., ReLU activations) directly into a MIP or satisfiability formulation. Tjeng et al. [12] formulate the verification of piecewise-linear neural networks as a mixed-integer linear program, enabling exact adversarial robustness checks with orders-of-magnitude speedups over earlier methods. Building on such encodings, Anderson et al. [13] developed stronger MILP formulations for ReLU-based networks, which further tighten the linear relaxations and improve solving efficiency. In parallel, practical frameworks have emerged to automate these integrations: for example, PySCIPOpt-ML [14] provides an interface to embed trained machine learning models (including neural nets) as constraints within the open-source solver SCIP [15]. These advances demonstrate the viability of treating a neural network as a combinatorial constraint, allowing exact optimization or formal verification involving network outputs.

However, existing approaches to neural network integration face fundamental limitations. A prevailing tactic is to *fully linearise* every activation, yielding a single, rigid MILP. Any change to the network then forces a complete reformulation; the encoding relies on large Big-M bounds [16–18] that weaken relaxations [19, 20]; and runtime soars with depth and width. In our largest test, translating a 64×512 ReLU model for 500 samples with PYSCIPOPT-ML inflates the problem from 500 variables to 5,900,000 variables and 7,800,000 constraints, yet SCIP still times out after two hours. Even the tighter formulations of Anderson et al. [13] remain highly size-sensitive. These limitations motivate a framework that **decouples** the neural and combinatorial parts, achieving

scalable, **modular**, and **adaptable** integration without loss of optimality.

We propose a **dual-decomposition** scheme that duplicates the integer vector x with a continuous copy u, relaxes the coupling equality u = x via an augmented-Lagrange term, and then alternates between two native solves: (i) a branch-and-cut MIP on x and (ii) a constrained first-order update on u. After each pair of solves the dual multipliers are updated, shrinking the mismatch until the two blocks agree; because neither block is ever reformulated into the language of the other, the method keeps the full power of specialised MILP engines and modern NN optimisers while sidestepping the Big-M explosion. This method yields three validated advantages. Scalability: On the X-Large case (6×128 ReLU, 500 samples) our dualdecomposition solver finishes in 8.7s, whereas PYSCIPOPT-ML needs 900s or more—a 100× speed-up obtained. Mod**ularity**: replacing the NN sub-solver (projected-gradient \leftrightarrow log-barrier) leaves the MIP untouched and changes total time by less than a factor of two. Adaptability: swapping the backbone MLP for a CNN or LSTM requires no reformulation and still converges in under 47s with the same objective value. Section VI details these results, confirming that dual decomposition can combine learning surrogates with discrete optimisation at scale.

Our main contributions are as follows:

- Algorithm. We introduce a dual-decomposition framework that couples a mixed-integer subproblem with a neural subproblem through an augmented-Lagrange split, avoiding any ${\rm Big-}M$ reformulation.
- **Theory.** We proof global convergence of the alternating scheme and prove that the per-iteration cost grows only linearly with network size, guaranteeing scalability by design.
- Experiments. Extensive experiments confirm that the solver is *scalable* (up to 100× faster than monolithic baselines), *modular* (sub-solvers can be swapped without code changes), and *adaptable* (CNN and LSTM backbones solve in < 47 s with identical optima).

II. PRELIMINARIES

a) Mixed Integer Linear Programming (MILP).: Given a set of decision variables $x \in \mathbb{R}^n$, the MILP problem is formulated as follow:

min
$$c^{\top} x$$
,
s.t. $Ax \ge b$, $l \le x \le u$, (1)
 $x \in \{0,1\}^p \times \mathbb{Z}^q \times \mathbb{R}^{n-p-q}$,

where $c \in \mathbb{R}^n$ is the objective coefficients, $A \in \mathbb{R}^{m \times n}$ is the constraint coefficient matrix, $b \in \mathbb{R}^m$ is the right-hand side vector, $l, u \in \mathbb{R}^n$ are the variable bounds.

b) Augmented Lagrangian Method (ALM).: We consider the equality-constrained problem as below:

$$\min_{x \in \mathbb{R}^n} f(x) \quad \text{s.t.} \quad c_i(x) = 0, \quad i \in \mathcal{E}, \tag{2}$$

where \mathcal{E} indexes the set of equality constraints. A straightforward quadratic-penalty approach enforces the constraints by minimising the following equation:

$$\Phi_k^{\text{pen}}(x) = f(x) + \mu_k \sum_{i \in \mathcal{E}} c_i(x)^2, \tag{3}$$

and gradually driving $\mu_k \to \infty$; however, large penalties typically induce severe ill-conditioning [21].

To mitigate this, the augmented Lagrangian augments the objective with a linear multiplier term as:

$$\Phi_k(x) = f(x) + \frac{\mu_k}{2} \sum_{i \in \mathcal{E}} c_i(x)^2 + \sum_{i \in \mathcal{E}} \lambda_i c_i(x), \quad (4)$$

where $\lambda \in \mathbb{R}^{|\mathcal{E}|}$ estimates the true Lagrange multipliers. At outer iteration k, one solves:

$$x^{(k)} = \arg\min_{x} \Phi_k(x),$$

then updates the multipliers by:

$$\lambda_i^{(k+1)} = \lambda_i^{(k)} + \mu_k c_i(x^{(k)}), \quad i \in \mathcal{E},$$
 (5)

and increases μ_k (e.g. $\mu_{k+1} = \beta \mu_k$ with $\beta > 1$) only when constraint violations stagnate. Because the linear term offsets part of the quadratic penalty, μ_k can stay moderate, leading to better numerical conditioning and stronger convergence guarantees. In practice, safeguards that bound λ are often used to prevent numerical overflow [22].

III. PROBLEM FORMULATION AND MOTIVATION

We study mixed-integer programmes (MIPs) that *embed* a pretrained neural network (NN) directly into their objective and constraints. Let $x \in \mathbb{Z}^p$ denote the discrete decisions and $y := f_{\theta}(x) \in \mathbb{R}^q$ the NN output; f_{θ} is differentiable with fixed parameters θ . The general problem is

$$\min_{x \in \mathbb{Z}^p} \quad c^{\top} x + d^{\top} y$$
s.t.
$$A \begin{bmatrix} x \\ y \end{bmatrix} \le b,$$

$$y = f_{\theta}(x).$$
(6)

with $c \in \mathbb{R}^p$ and $d \in \mathbb{R}^q$ weighting the discrete cost and the NN-dependent cost, $A \in \mathbb{R}^{m \times (p+q)}$ and $b \in \mathbb{R}^m$ capturing all affine limits that jointly constrain the decisions and the NN prediction. Because the mapping $x \mapsto y = f_{\theta}(x)$ is nonlinear, problem (6) inherits both the combinatorial hardness of MIPs and the nonlinearity of deep networks, making it particularly challenging to solve.

a) Limitations of Network-to-MIP Embedding.: A common strategy for incorporating a pretrained NN into a MIP is to replace each nonlinear operation by piecewise-linear surrogates—e.g. Big-M formulations [23] or SOS1 constraints [24]. Although exact, these encodings introduce $\mathcal{O}(Lh)$ additional binaries and constraints for an L-layer, h-unit MLP, which can blow up the solver's search tree even for moderate network sizes. Moreover, available linearization routines support only basic primitives (dense ReLUs, simple max-pooling), whereas

modern architectures—convolutional filters, recurrent gates, attention blocks and layer-normalisation—have no off-the-shelf encodings. Adapting each novel layer requires bespoke linearization, increasing modelling complexity and hindering extensibility.

b) Rationale for Decomposition.: By contrast, treating the NN as a black-box oracle avoids this overhead but sacrifices explicit feasibility guarantees, risking violations of critical constraints in safety-sensitive applications. To overcome the computational challenges associated with monolithic linearization approaches, we propose employing augmented Lagrangian decomposition. This technique partitions the original problem (6) into simpler subproblems, each handled by specialized solvers, while iteratively maintaining solution consistency through dual updates. This decomposition approach provides significant computational advantages, improved scalability, and robust theoretical convergence properties.

IV. OUR DECOMPOSITION-BASED METHOD

We introduce an auxiliary continuous variable $u \in \mathbb{R}^p$ to duplicate the integer variable x, resulting in an equivalent but more tractable formulation featuring explicit coupling constraints:

$$\min_{x,u} \quad c^{\top} x + d^{\top} f_{\theta}(u)
\text{s.t.} \quad A_{\text{MIP}} x \leq b_{\text{MIP}},
\quad A_{\text{NN}} \begin{bmatrix} u \\ f_{\theta}(u) \end{bmatrix} \leq b_{\text{NN}},
\quad u = x, \quad x \in \mathbb{Z}^{p}.$$
(7)

Here $A_{\mathrm{MIP}} \in \mathbb{R}^{m_1 \times p}$, $b_{\mathrm{MIP}} \in \mathbb{R}^{m_1}$ store the "legacy" linear limits that involve only the integer vector x. All remaining affine constraints that depend on the NN output are written as $A_{\mathrm{NN}} \in \mathbb{R}^{m_2 \times (p+q)}$ and $b_{\mathrm{NN}} \in \mathbb{R}^{m_2}$ acting on the stacked vector $[u; f_{\theta}(u)]$. Across iterations u stays continuous—enabling inexpensive first-order updates of the NN block—while the coupling equation u = x is enforced at convergence to recover a valid integer solution.

A. High-Level Decomposition Approach

The key theoretical challenge we address is the nonconvex equality constraint u=x. We handle this complexity by introducing dual multipliers (Lagrange multipliers) $\lambda \in \mathbb{R}^p$ and a quadratic penalty term controlled by parameter $\rho>0$. The resulting augmented Lagrangian function is given by:

$$\mathcal{L}_{\rho}(x, u, \lambda) = c^{\top} x + d^{\top} f_{\theta}(u) + \lambda^{\top} (u - x) + \frac{\rho}{2} \|u - x\|_{2}^{2}.$$
 (8)

The term $\lambda^{\top}(u-x)$ is the *classical* Lagrange coupling: at a Karush-Kuhn-Tucker(KKT) point [25] it drives the equality u=x by adjusting the dual multipliers, while supplying first-order information to each subproblem. The quadratic addon $\frac{\rho}{2}\|u-x\|_2^2$ augments the Lagrangian, injecting strong convexity that damps oscillations and markedly accelerates the alternating updates observed in practice. The penalty

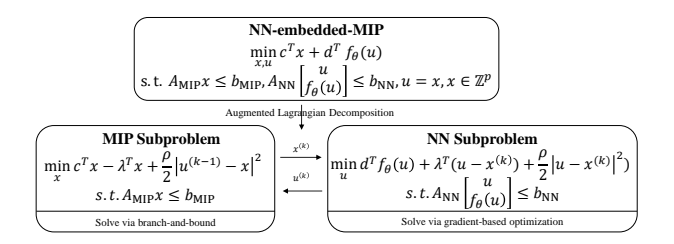


Fig. 2. Illustration of the proposed NN-embedded MIP solution framework using augmented Lagrangian decomposition, emphasizing iterative primal-dual coordination.

weight $\rho>0$ balances two competing objectives: (i) allowing the MIP and NN blocks enough flexibility to explore their individual feasible regions (small ρ), and (ii) tightening the coupling to secure rapid primal feasibility (large ρ). Following standard augmented-Lagrangian heuristics [26], we initialize ρ conservatively and increase it adaptively whenever the primal residual $\|u-x\|_2$ ceases to decrease, thereby achieving both robustness and efficiency. Figure 2 illustrates our proposed dual decomposition workflow, highlighting the iterative, coordinated solving of the decomposed subproblems. Algorithm 1 provides the pseudocode.

Algorithm 1 Dual Decomposition for NN-Embedded MIP

Require: Initialization $u^{(0)}, \lambda^{(0)}, \rho > 0$, tolerance ε , maximum iterations K

- 1: **for** k = 1, ..., K **do**
- 2: Solve MIP subproblem for $x^{(k)}$ to update discrete decisions.
- 3: Solve NN subproblem (PGD or Log-Barrier) for $u^{(k)}$ to refine continuous inputs.
- 4: Update dual multiplier: $\lambda^{(k)} \leftarrow \lambda^{(k-1)} + \rho(u^{(k)} x^{(k)})$.
- 5: Check convergence: if $||u^{(k)} x^{(k)}||_{\infty} < \varepsilon$, terminate.
- 6: Adjust penalty parameter ρ adaptively based on residuals.
- 7: end for
- 8: **return** optimal solution pair (x^*, u^*) .

B. Detailed Modular Subproblem Decomposition

We then decompose the augmented Lagrangian into two tractable subproblems solved alternately and coordinated by iterative updates of the dual multipliers:

a) MIP Subproblem.: Given $(u^{(k-1)}, \lambda^{(k-1)})$, the MIP subproblem is defined as:

$$\begin{split} x^{(k)} &= \arg\min_{x \in \mathbb{Z}^p} \left(c^\top x - \lambda^{(k-1)\top} x + \frac{\rho}{2} \left\| u^{(k-1)} - x \right\|_2^2 \right) \\ \text{s.t.} \quad A_{\text{MIP}} \, x \, \leq \, b_{\text{MIP}}. \end{split} \tag{9}$$

This formulation retains the linear constraints $A_{\text{MIP}} x \leq b_{\text{MIP}}$ but adjusts the objective to include the penalty term $\|u^{(k-1)} - x\|_2^2$, thereby encouraging proximity between x and the current NN solution $u^{(k-1)}$. It includes the linear term $-\lambda^{(k-1)\top} x$, the Lagrange multiplier contribution originating from the

coupling constraint u=x in the augmented Lagrangian. The companion constant $\lambda^{(k-1)\top}u^{(k-1)}$ is omitted because it is independent of x and thus irrelevant for the minimisation. Modern branch-and-bound or cutting-plane solvers [27, 28] can efficiently handle this subproblem due to its convexified structure [29].

b) NN Subproblem.: Given the discrete solution $x^{(k)}$ and multiplier $\lambda^{(k-1)}$, the continuous variables are optimized through solving:

$$u^{(k)} = \arg\min_{u \in \mathbb{R}^p} \left\{ d^{\top} f_{\theta}(u) + \lambda^{(k-1)\top} \left(u - x^{(k)} \right) + \frac{\rho}{2} \|u - x^{(k)}\|_2^2 \right\}$$

$$\text{s.t.} \quad A_{\text{NN}} \begin{bmatrix} u \\ f_{\theta}(u) \end{bmatrix} \leq b_{\text{NN}}.$$

$$(10)$$

Fixing the discrete iterate $x^{(k)}$ isolates the continuous decision u, letting us recalibrate the neural input without perturbing the combinatorial block. The first term $d^{\top}f_{\theta}(u)$ transmits the original cost coefficients to the NN, while the dual inner product $\lambda^{(k-1)\top}(u-x^{(k)})$ conveys the mismatch detected in the preceding coordination step. The proximal penalty $\frac{\rho}{2}\|u-x^{(k)}\|_2^2$ tempers aggressive updates, yielding a well-conditioned landscape. Crucially, the stacked linear constraint $A_{\rm NN}\left[u\;;\;f_{\theta}(u)\right]\leq b_{\rm NN}$ preserves every safety or performance limit originally imposed on the network output, ensuring that each neural adjustment remains admissible before the next dual synchronization.

C. Solving the NN Subproblem with Constraints

The NN subproblem is non-trivial due to the nonlinear nature of $f_{\theta}(u)$ and the constraint $A_{\rm NN}[\,u\,\,;\,\,f_{\theta}(u)] \leq b_{\rm NN},$ which induces the feasible set

$$\mathcal{C} \ := \ \Big\{ u \in \mathbb{R}^p \ \Big| \ A_{\mathrm{NN}} \left[\begin{matrix} u \\ f_{\theta}(u) \end{matrix} \right] \leq b_{\mathrm{NN}} \Big\}.$$

- a) Projected Gradient Descent (PGD).: When projection onto $\mathcal C$ is affordable—e.g., if $A_{\rm NN}$ encodes simple box or monotone limits—we perform
 - 1) a gradient step on the smooth part of the objective, then
 - 2) an orthogonal projection back onto C.

Let $J_{f_{\theta}}(u)$ denote the Jacobian of f_{θ} at u. The gradient of the augmented Lagrangian with fixed $(x^{(k)}, \lambda^{(k-1)})$ reads

$$\nabla_{u} \mathcal{L}_{\rho}(u) = J_{f_{\theta}}(u)^{\top} d + \lambda^{(k-1)} + \rho (u - x^{(k)}).$$

With stepsize $\eta > 0$ we update

$$u \leftarrow \operatorname{Proj}_{\mathcal{C}}(u - \eta \nabla_u \mathcal{L}_{\rho}(u)),$$

where $\operatorname{Proj}_{\mathcal{C}}$ is the Euclidean projection [30] onto \mathcal{C} . The proximal term $\rho \|u - x^{(k)}\|_2^2$ ensures the landscape is well-conditioned, and PGD typically converges in a handful of iterations [31].

b) Log-Barrier Interior Method.: If projection is itself expensive (e.g. C is defined by many affine cuts on f_{θ}), we instead absorb the constraints via a logarithmic barrier:

$$\min_{u \in \mathbb{R}^p} \left\{ d^{\top} f_{\theta}(u) + \lambda^{(k-1)\top} (u - x^{(k)}) + \frac{\rho}{2} \|u - x^{(k)}\|_{2}^{2} - \mu \sum_{j=1}^{m} \log \left(b_{\text{NN},j} - a_{j}^{\top} \begin{bmatrix} u \\ f_{\theta}(u) \end{bmatrix} \right) \right\}$$

where a_j^{\top} is the j-th row of $A_{\rm NN}$ and $\mu>0$ is the barrier parameter. Starting from a strictly feasible point, we solve the above with a second-order method and gradually decrease μ ($\mu\!\leftarrow\!0.1\mu$) until the dual feasibility tolerance is reached. This interior-point strategy dispenses with explicit projections yet retains strict feasibility along the entire Newton path [32]; it is especially beneficial when $\mathcal C$ is described by many coupled linear cuts but occupies a relatively low-volume region, where projection costs dominate.

D. Dual Updates and Penalty Parameter Adjustments

The dual multipliers are iteratively updated to maintain primal-dual feasibility:

$$\lambda^{(k)} \leftarrow \lambda^{(k-1)} + \rho(u^{(k)} - x^{(k)}).$$
 (11)

The penalty parameter ρ is dynamically adjusted to effectively balance primal feasibility and dual optimization stability:

- Increasing ρ enhances primal feasibility enforcement when constraint violations persist.
- Decreasing ρ accelerates convergence by mitigating slow dual updates or numerical instability.

V. THEORETICAL ANALYSIS

In this section, we provide two theoretical perspectives on our proposed decomposition framework: (i) a convergence analysis showing that our primal-dual scheme yields globally convergent iterates under standard assumptions; and (ii) a scalability analysis demonstrating that the computational complexity of our method grows only linearly with the neural network size, ensuring robust performance as problem instances scale.

A. Convergence Analysis

We prove that Algorithm 1 converges to a KKT point of the augmented Lagrangian.

Assumption 1. 1) $\mathcal{X} := \{x \in \mathbb{Z}^p \mid A_{MIP}x \leq b_{MIP}\}$ is non-empty and bounded;

- 2) The map $g(u) := d^{\top} f_{\theta}(u)$ is convex and has L-Lipschitz gradient (L-smooth);
- 3) $C := \{u \mid A_{NN}[u; f_{\theta}(u)] \leq b_{NN}\}$ is non-empty and satisfies Slater's condition;
- 4) A penalty $\rho > L$ is chosen once (or increased finitely many times and then fixed).

Theorem V.1 (Convergence to a KKT point). Under Assumption 1, the sequence $\{(x^{(k)}, u^{(k)}, \lambda^{(k)})\}$ generated by

Algorithm 1 is bounded. Every accumulation point (x^*, u^*, λ^*) satisfies:

$$u^{\star} = x^{\star},$$

$$\nabla_{u} \mathcal{L}_{\rho}(x^{\star}, u^{\star}, \lambda^{\star}) = 0,$$

$$x^{\star} \in \arg\min_{x \in \mathcal{X}} \mathcal{L}_{\rho}(x, u^{\star}, \lambda^{\star}).$$
(12)

Moreover,

$$\min_{t \le k} \|u^{(t)} - x^{(t)}\|_{2}^{2} = \mathcal{O}(\frac{1}{k}),$$

$$\mathcal{L}_{\rho}(x^{(k)}, u^{(k)}, \lambda^{(k)}) - \mathcal{L}_{\rho}(x^{\star}, u^{\star}, \lambda^{\star}) = \mathcal{O}(\frac{1}{k}).$$
(13)

Proof. The argument proceeds in three steps. (i) Descent in the u-block. Because $g(u) = d^{\top} f_{\theta}(u)$ is L-smooth and $\rho > L$, the function $g(u) + \frac{\rho}{2} ||u - x||_2^2$ is $(\rho - L)$ strongly convex in u. Solving the NN subproblem exactly therefore yields a strict decrease in the augmented merit and a bound of order $||u^{(k)} - x^{(k-1)}||_2^2$. (ii) Descent in the x-block. The discrete set \mathcal{X} is finite and each MIP subproblem is solved to global optimality, so minimisation over x never increases the augmented Lagrangian. (iii) Dual update. Updating $\lambda^{(k+1)} = \lambda^{(k)} + \rho(u^{(k)} - x^{(k)})$ produces the telescoping identity $\mathcal{M}_{\rho}^{(k+1)} = \mathcal{M}_{\rho}^{(k)} - \frac{\rho - L}{2} \|u^{(k)} - x^{(k)}\|_2^2$, so $\sum_k \|u^{(k)} - x^{(k)}\|_2^2 < \infty$ and $\min_{t \le k} \|u^{(t)} - x^{(t)}\|_2^2 = \mathcal{O}(1/k)$. The merit is bounded below, hence the iterate sequence is bounded; by Bolzano-Weierstrass it has accumulation points, and the first-order optimality of both exact subsolvers implies every such point satisfies the KKT system. Full details are deferred to Appendix.

B. Scalability with Neural Network Size

Next, we analyze how the complexity of our method scales with the neural network architecture.

Theorem V.2 (Linear Scalability in Network Size). Let P denote the number of parameters in the neural network f_{θ} . Then each iteration of Algorithm 1 has overall complexity

$$\mathcal{O}(T_{MIP} + P), \tag{14}$$

where T_{MIP} is the complexity of solving the MIP subproblem, independent of P. Consequently, for fixed MIP size, the runtime per iteration grows linearly with the network size.

Proof. (i) The MIP subproblem (9) depends only on x, λ , and $u^{(k-1)}$; its size does not increase with P. Thus, T_{MIP} is independent of the neural architecture. (ii) The NN subproblem (10) requires evaluating $f_{\theta}(u)$ and its Jacobian $J_{f_{\theta}}(u)$. For standard feedforward networks, forward and backward passes both require $\mathcal{O}(P)$ time [33]. (iii) The projection or barrier operations involve only affine constraints A_{NN} , whose size is fixed by the problem specification and independent of P. Therefore, the per-iteration complexity is $\mathcal{O}(T_{\text{MIP}} + P)$, implying linear scaling with the network size.

In a Big-M linearisation, every hidden unit contributes a constant number of *additional variables and constraints*, so the model dimension itself grows roughly linearly with network

depth and width. However, the resulting MILP remains NP-hard; empirical and worst-case studies show that solver time rises super-linearly, often exponentially, with that dimension increase [34]. By leaving the network outside the MILP, our decomposition sidesteps this blow-up and retains per-iteration linear scaling.

VI. EXPERIMENTAL EVALUATIONS

Overview of Experiments. We perform five complementary studies to thoroughly evaluate the proposed dual-decomposition framework: (E1) a head-to-head comparison with Big-M linearisation; (E2) a stress test that scales network depth and width; (E3) an ablation that removes the dual-update loop; (E4) a modularity study that swaps heterogeneous network architectures without changing solver logic; and (E5) a subsolver comparison between projected-gradient descent and a log-barrier interior method. Together, these experiments probe solution quality, runtime efficiency, robustness, architecture agnosticism, and the impact of continuous-block solver choice.

A. Experimental Setup

1) Implementation Details.: All experiments are implemented in Python: neural classifiers are trained with PyTorch [35], while MIP subproblems are solved via Pyscipopt 8.0.4 [36]. For the linearisation baseline, we use PYSCIPOPT-ML to linearise the trained classifier via its Big-M add_predictor_constr interface. For dual **decomposition (DD)**, we adopt an ADMM-style scheme with $\rho = 10.0$, step size $\eta = 0.01$, and convergence tolerance $\varepsilon = 10^{-4}$. Each augmented-Lagrange iteration first solves the MIP subproblem, then refines the neural block—performing 25 Adam [37] steps in the PGD variant or an L-BFGS-B [38] update in the log-barrier variant. Experiments E1-E4 solve the neural subproblem with the PGD variant. We allow at most 50 iterations and enforce a per-instance time budget of 300 s. Every configuration is executed under five random seeds $\{42, 123, 456, 789, 1024\}$ and we report averages. All experiments are conducted on a single machine equipped with eight NVIDIA GeForce RTX 4090 GPUs and two AMD EPYC 7763 CPUs.

2) Dataset.: (1) Water Potability. Used in Experiments E1–E4. The dataset offers ne water-quality features with binary drinkability labels. From the undrinkable subset we draw instances of size $n \in \{25, 50, 100, 200, 400\}$. Each optimisation task selects feature adjustments—subject to perfeature budgets of ± 2.0 —to maximise the number of samples classified as potable. (2) Tree Planting [39]. Employed exclusively in Experiment E5 for the subsolver comparison. Four species placed on an $n_{\rm grid} \times n_{\rm grid}$ plot ($n_{\rm grid} = 6$). Seven site features feed neural survival models. Dual decomposition (PGD and log-barrier) is compared to a Big-M baseline.

B. (E1) Comparison with Linearisation-based Methods

We benchmark DD against the Big-M linearisation in PYSCIPOPT-ML on four configurations—Small (2×16),

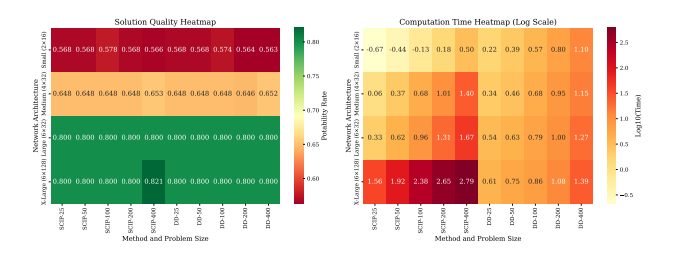


Fig. 3. (E1) Comparison with Linearisation-based Methods. Solution quality (left) and computation time (right) across network architectures and problem sizes. Colours denote potability rate and \log_{10} wall-clock time, respectively.

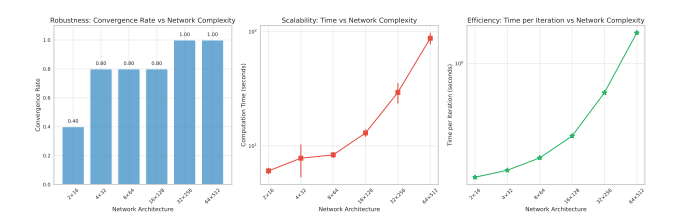


Fig. 4. (E2) Scalability stress test with fixed n=100. Left: convergence rate; centre: total computation time (log scale); right: average time per iteration (log scale).

Medium (4 \times 32), Large (6 \times 64), and X-Large (6 \times 128)—and five instance sizes.

Solution Quality. DD aligns with the monolithic baseline across all configurations (Fig. 3, left), evidencing virtually no performance loss from decomposition on this task. **Computation Time.** Big-M runtimes exceed 10^2 s as depth or n grows, whereas DD stays near 10 s even on the hardest cases, delivering $10-100 \times$ speed-ups (Fig. 3, right).

C. (E2) Scalability Stress Test Across Network Depth

We fix the sample size at n=100 and sweep six increasingly deep MLPs 0 , repeating each configuration over five random seeds. For every run we record (i) success rate within 50 DD iterations, (ii) total wall-clock time, and (iii) average time per iteration.

Robustness. Only 40% of the 2×16 runs converge within the 50-iteration cap, yet every network at or beyond 16×128 succeeds in all trials (Fig. 4, left). **Scalability.** Total solve time grows with depth but remains under $90\,\mathrm{s}$ even for the 64×512 model (Fig. 4, centre). **Efficiency.** Per-iteration cost increases sub-linearly with network size (Fig. 4, right), implying that the extra overhead stems chiefly from neural evaluation, not the optimisation loop. For reference, PYSCIPOPT-ML fails beyond the 6×128 (X-Large) model: deeper nets either exceed memory limits or time out at $300\,\mathrm{s}$. DD therefore avoids the prohibitive linearisation burden through its decomposition strategy.

D. (E3) Ablation Study: Impact of Dual Coordination

To quantify the contribution of the dual-update mechanism we construct a degenerate variant—single-step gradi-

 $^{0}2\times16,\ 4\times32,\ 8\times64,\ 16\times128,\ 32\times256,\ 64\times512$ hidden units.

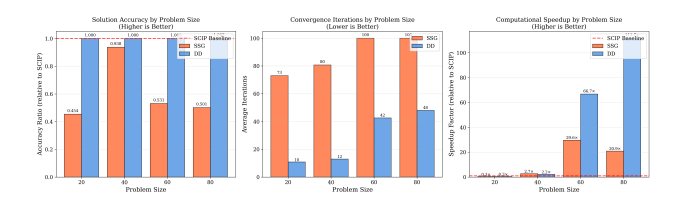


Fig. 5. (E3) **Ablation results.** SSG (no dual coordination) versus full DD. Left: solution quality (normalised to SCIP). Centre: *log* average iterations to feasibility. Right: speed-ups over SCIP (higher is better).

ent (SSG)—that performs one projected-gradient step on u, heuristically rounds to an integer x, and terminates. The design is inspired by the direct gradient-descent solver of DIFFILO [40], which tackles NN-embedded MIPs without dual variables, and the complete SSG pseudocode is given in Appendix. Powers-of-two instance sizes $(n \in \{32, 64, 128\})$ are chosen for clearer logarithmic plots.

- Solution quality. SSG attains erratic accuracies—0.45, 0.94, 0.53, and 0.50 of the SCIP benchmark as n grows—whereas DD stays at unity (and even 0.998 for n=80), confirming that the decomposition preserves optimality.
- Convergence. SSG requires 73-100 iterations (avg. \approx 88), often stalling at the cap; DD converges in an average of 10, 12, 42, and 48 iterations for n=20,40,60,80, respectively, underscoring the stabilising effect of the dual updates.
- **Runtime.** SSG is slower than SCIP for n=20 $(0.3\times)$, modestly faster for n=40 $(2.7\times)$, and reaches $20-30\times$ speed-ups at larger scales. DD starts on par with SSG at n=40 $(2.2\times)$, then widens the gap to $66.7\times$ and $111.7\times$ for n=60 and 80, respectively.

Dual coordination is indispensable: removing it degrades numerical robustness, inflates iteration counts by two-three orders of magnitude, and erodes the runtime advantage as n increases. Alternating dual updates are therefore critical for both rapid convergence and high-quality solutions.

E. (E4) Adaptability Across Neural Architectures

We run the *unchanged* DD solver on four disparate predictors: a shallow fully connected network (FC), a lightweight CONV1D, a deep RESNET, and a sequential LSTM. By contrast, linearisation frameworks such as PYSCIPOPT-ML only support simple feed-forward layers and cannot encode CNN or LSTM backbones at all.

- Predictive fidelity. DD preserves the original accuracies: 0.694 (FC), 0.743 (CONV1D), 0.791 (LSTM), and 0.696 (RESNET), demonstrating zero distortion of the learned models.
- Convergence across backbones. Within the 50-iteration limit DD satisfies $\|u-x\|_{\infty} < 10^{-4}$ in 0.83 of CONV1D runs, 0.75 of FC runs, 0.83 of RESNET runs, and 0.50

¹Identical to Algorithm 1 but with the dual update removed and $\lambda = \rho = 0$.

- of LSTM runs—architectures that existing linearisation tool-chains cannot even represent.
- Scalable runtime. At the largest problem size (n=200) average solve times are $\approx 6 \, \mathrm{s}$ (FC), $\approx 8 \, \mathrm{s}$ (RESNET), $\approx 15 \, \mathrm{s}$ (CONV1D), and $\approx 50 \, \mathrm{s}$ (LSTM), all well inside the $300 \, \mathrm{s}$ wall-clock timeout where linearised formulations already fail.

F. (E5) Modular Subsolver Test: PGD vs. Log-Barrier

We verify the plug-and-play nature of our framework by fixing all outer-loop parameters ($\rho=10$, 50 iterations, stopping criterion) and only swapping the NN subsolver: **DD-PGD** (25 Adam steps with projection) versus **DD-Barrier** (damped Newton on a log-barrier with five CG steps, $\mu \leftarrow 0.1\mu$). The monolithic linearisation baseline (SCIP) is included for reference.

Results (Fig. 7) exhibit a three-tier structure: SCIP-ML escalates from 111 s to 860 s; DD-Barrier completes in 8.5s, 24.8s and 63.1s (13–16× speed-ups); DD-PGD runs in 0.4s, 1.4s and 6.5s (130–280× speed-ups over SCIP, 9–21× over Barrier). Preservation of identical classification accuracy confirms that these gaps stem purely from the continuous-solver choice. This isolated subsolver swap—without any change to the MIP block, dual updates or data handling—demonstrates true modularity: users can interchange NN optimisation routines to match constraint complexity (e.g. cheap projection vs. dense polyhedral limits) while retaining all theoretical and empirical benefits of the dual-decomposition framework.

G. Summary of Findings

Across five studies we establish three main results. (i) Scalability: DD maintains near-optimal quality while delivering $10 \times -280 \times$ speed-ups over Big-M linearisation (E1, E2). (ii) Necessity of dual updates: removing them degrades accuracy by up to 55% and inflates iteration counts by two orders of magnitude (E3). (iii) Modularity & Adaptability: DD functions as a plug-and-play layer—handling CNN, LSTM backbones and interchangeable PGD/Barrier sub-solvers without code changes—yet still outperforms linearisation baselines by at least an order of magnitude (E4, E5). These empirical results corroborate the theoretical claims of Section I and demonstrate that dual decomposition offers a practical path to embedding complex neural surrogates in large-scale mixed-integer optimisation.

VII. CONCLUSION

We proposed a modular and scalable dual decomposition framework for integrating neural networks into mixed-integer optimization, enabling principled coordination between learning-based models and combinatorial solvers without requiring explicit constraint encodings. Our method outperforms monolithic baselines in both runtime and flexibility across a range of problem sizes and neural architectures. Despite its advantages, several limitations remain. First, the convergence rate can be sensitive to hyperparameters such as the penalty ρ and step size, suggesting the need for adaptive or

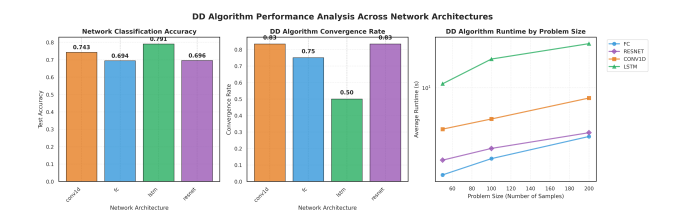


Fig. 6. (E4) Adaptability across architectures. Left: stand-alone test accuracy. Centre: fraction of DD runs (five seeds) converging within the 50-iteration cap. Right: geometric-mean runtime (log scale) for $n \in \{60, 100, 200\}$.

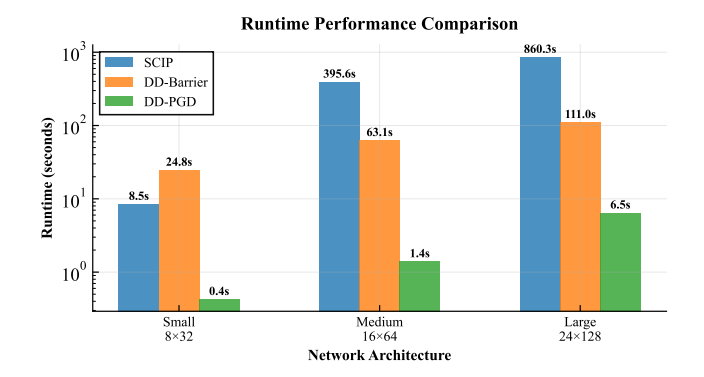


Fig. 7. (E5) **Modular subsolver test.** Wall–clock runtime (log scale) for DD-PGD, DD-Barrier, and the linearisation baseline on the *Small* (8×32) , *Medium* (16×64) , and *Large* (24×128) MLPs.

learned scheduling strategies. Second, our framework currently assumes access to gradient information from the neural network; extending to non-differentiable or black-box predictors remains an open challenge. Finally, while we focus on a single network, many real-world problems involve multiple interacting predictors or dynamic decision feedback, which could be explored via multi-block decomposition or hierarchical coordination.

ACKNOWLEDGMENTS

The research is partially supported by Quantum Science and Technology-National Science and Technology Major Project (QNMP) 2021ZD0302900 and China National Natural Science Foundation with No. 62132018, 62231015, "Pioneer" and "Leading Goose" R&D Program of Zhejiang", 2023C01029, and 2023C01143.

REFERENCES

- [1] Y. Bengio, A. Lodi, and A. Prouvost, "Machine learning for combinatorial optimization: a methodological tour d'horizon," *European Journal of Operational Research*, vol. 290, no. 2, pp. 405–421, 2021.
- [2] Q. Cappart, T. Moisan, L.-M. Rousseau, I. Prémont-Schwarz, and A. A. Cire, "Combining reinforcement learning and constraint programming for combinatorial optimization," in *Proceedings of the AAAI conference on artificial intelligence*, vol. 35, no. 5, 2021, pp. 3677–3687.

- [3] A. V. Joshi, "Machine learning and artificial intelligence," 2020.
- [4] D. Bertsimas, A. O'Hair, S. Relyea, and J. Silberholz, "An analytics approach to designing combination chemotherapy regimens for cancer," *Management Science*, vol. 62, no. 5, pp. 1511–1531, 2016.
- [5] M. S. Misaghian, G. Tardioli, A. G. Cabrera, I. Salerno, D. Flynn, and R. Kerrigan, "Assessment of carbon-aware flexibility measures from data centres using machine learning," *IEEE Transactions on Industry Applications*, vol. 59, no. 1, pp. 70–80, 2022.
- [6] J. Jalving, J. Ghouse, N. Cortes, X. Gao, B. Knueven, D. Agi, S. Martin, X. Chen, D. Guittet, R. Tumbalam-Gooty et al., "Beyond price taker: Conceptual design and optimization of integrated energy systems using machine learning market surrogates," *Applied Energy*, vol. 351, p. 121767, 2023.
- [7] S. Droste, T. Jansen, and I. Wegener, "Upper and lower bounds for randomized search heuristics in black-box optimization," *Theory of computing systems*, vol. 39, no. 4, pp. 525–544, 2006.
- [8] F. Ceccon, J. Jalving, J. Haddad, A. Thebelt, C. Tsay, C. D. Laird, and R. Misener, "Omlt: Optimization & machine learning toolkit," *Journal of Machine Learning Research*, vol. 23, no. 349, pp. 1–8, 2022.
- [9] D. Bergman, T. Huang, P. Brooks, A. Lodi, and A. U. Raghunathan, "Janos: an integrated predictive and prescriptive modeling framework," *INFORMS Journal on Computing*, vol. 34, no. 2, pp. 807–816, 2022.
- [10] M. Lombardi, M. Milano, and A. Bartolini, "Empirical decision model learning," *Artificial Intelligence*, vol. 244, pp. 343–367, 2017.
- [11] D. Maragno, H. Wiberg, D. Bertsimas, Ş. İ. Birbil, D. den Hertog, and A. O. Fajemisin, "Mixed-integer optimization with constraint learning," *Operations Research*, vol. 73, no. 2, pp. 1011–1028, 2025.
- [12] V. Tjeng, K. Xiao, and R. Tedrake, "Evaluating robustness of neural networks with mixed integer programming," *arXiv preprint arXiv:1711.07356*, 2017.
- [13] R. Anderson, J. Huchette, W. Ma, C. Tjandraatmadja, and J. P. Vielma, "Strong mixed-integer programming formulations for trained neural networks," *Mathematical Programming*, vol. 183, no. 1, pp. 3–39, 2020.
- [14] M. Turner, A. Chmiela, T. Koch, and M. Winkler, "Pyscipopt-ml: Embedding trained machine learning models into mixed-integer programs," *arXiv* preprint *arXiv*:2312.08074, 2023.
- [15] K. Bestuzheva, M. Besançon, W.-K. Chen, A. Chmiela, T. Donkiewicz, J. Van Doornmalen, L. Eifler, O. Gaul, G. Gamrath, A. Gleixner et al., "Enabling research through the scip optimization suite 8.0," ACM Transactions on Mathematical Software, vol. 49, no. 2, pp. 1–21, 2023.
- [16] B. Grimstad and H. Andersson, "Relu networks as surrogate models in mixed-integer linear programs," *Comput*ers & Chemical Engineering, vol. 131, p. 106580, 2019.

- [17] J. Huchette, G. Muñoz, T. Serra, and C. Tsay, "When deep learning meets polyhedral theory: A survey," *arXiv* preprint arXiv:2305.00241, 2023.
- [18] F. Badilla, M. Goycoolea, G. Muñoz, and T. Serra, "Computational tradeoffs of optimization-based bound tightening in relu networks," arXiv preprint arXiv:2312.16699, 2023.
- [19] I. Griva, S. G. Nash, and A. Sofer, *Linear and nonlinear optimization 2nd edition*. SIAM, 2008.
- [20] J. D. Camm, A. S. Raturi, and S. Tsubakitani, "Cutting big m down to size," *Interfaces*, vol. 20, no. 5, pp. 61–66, 1990.
- [21] D. P. Bertsekas, Constrained optimization and Lagrange multiplier methods. Academic press, 2014.
- [22] M. R. Hestenes, "Multiplier and gradient methods," *Journal of optimization theory and applications*, vol. 4, no. 5, pp. 303–320, 1969.
- [23] M. Cococcioni and L. Fiaschi, "The big-m method with the numerical infinite m," *Optimization Letters*, vol. 15, no. 7, pp. 2455–2468, 2021.
- [24] T. Fischer and M. E. Pfetsch, "Branch-and-cut for linear programs with overlapping sos1 constraints," *Mathematical Programming Computation*, vol. 10, no. 1, pp. 33–68, 2018.
- [25] G. Gordon and R. Tibshirani, "Karush-kuhn-tucker conditions," *Optimization*, vol. 10, no. 725/36, p. 725, 2012.
- [26] T. Larsson and D. Yuan, "An augmented lagrangian algorithm for large scale multicommodity routing," *Computational Optimization and Applications*, vol. 27, no. 2, pp. 187–215, 2004.
- [27] K. Bestuzheva, M. Besançon, W.-K. Chen, A. Chmiela, T. Donkiewicz, J. Van Doornmalen, L. Eifler, O. Gaul, G. Gamrath, A. Gleixner *et al.*, "The scip optimization suite 8.0," *arXiv preprint arXiv:2112.08872*, 2021.
- [28] Gurobi Optimization, LLC, "Gurobi Optimizer Reference Manual," 2024. [Online]. Available: https://www.gurobi.com
- [29] M. Mistry, D. Letsios, G. Krennrich, R. M. Lee, and R. Misener, "Mixed-integer convex nonlinear optimization with gradient-boosted trees embedded," *INFORMS Journal on Computing*, vol. 33, no. 3, pp. 1103–1119, 2021.
- [30] J. Liu and J. Ye, "Efficient euclidean projections in linear time," in *Proceedings of the 26th annual international conference on machine learning*, 2009, pp. 657–664.
- [31] S. H. Haji and A. M. Abdulazeez, "Comparison of optimization techniques based on gradient descent algorithm: A review," *PalArch's Journal of Archaeology of Egypt/Egyptology*, vol. 18, no. 4, pp. 2715–2743, 2021.
- [32] M. Toussaint, "A tutorial on newton methods for constrained trajectory optimization and relations to slam, gaussian process smoothing, optimal control, and probabilistic inference," *Geometric and numerical foundations of movements*, pp. 361–392, 2017.
- [33] I. Goodfellow, Y. Bengio, A. Courville, and Y. Bengio, *Deep learning.* MIT press Cambridge, 2016, vol. 1,

- no. 2.
- [34] R. E. Bixby, "Implementing the simplex method: The initial basis," *ORSA Journal on Computing*, vol. 4, no. 3, pp. 267–284, 1992.
- [35] A. Paszke, S. Gross, F. Massa, A. Lerer, J. Bradbury, G. Chanan, T. Killeen, Z. Lin, N. Gimelshein, L. Antiga *et al.*, "Pytorch: An imperative style, high-performance deep learning library," *Advances in neural information processing systems*, vol. 32, 2019.
- [36] S. Maher, M. Miltenberger, J. P. Pedroso, D. Rehfeldt, R. Schwarz, and F. Serrano, "PySCIPOpt: Mathematical programming in python with the SCIP optimization suite," in *Mathematical Software – ICMS 2016*. Springer International Publishing, 2016, pp. 301–307.
- [37] D. P. Kingma and J. Ba, "Adam: A method for stochastic optimization," *arXiv preprint arXiv:1412.6980*, 2014.
- [38] C. Zhu, R. H. Byrd, P. Lu, and J. Nocedal, "Algorithm 778: L-bfgs-b: Fortran subroutines for large-scale boundconstrained optimization," ACM Transactions on mathematical software (TOMS), vol. 23, no. 4, pp. 550–560, 1997.
- [39] K. E. Wood, R. K. Kobe, I. Ibáñez, and S. McCarthy-Neumann, "Tree seedling functional traits mediate plantsoil feedback survival responses across a gradient of light availability," *Plos one*, vol. 18, no. 11, p. e0293906, 2023.
- [40] Z. Geng, J. Wang, X. Li, F. Zhu, J. Hao, B. Li, and F. Wu, "Differentiable integer linear programming," in The Thirteenth International Conference on Learning Representations, 2025.

APPENDIX

A. Baseline Algorithms

- 1) AutoLinearized: Exact Big-M Formulation:
- a) Rationale.: AutoLinearized follows the exact embedding paradigm: every nonlinear activation is rewritten as a mixed-integer linear block, so the original objective plus the network becomes a single MILP. A modern solver can then certify global optimality.
- b) Construction.: For a ReLU network we introduce a continuous output variable z_ℓ and a binary indicator y_ℓ for each hidden unit; the ReLU $s = \max\{0, h\}$ is replaced by

$$s \ge h, \qquad s \le h - M_1(1 - y), \tag{15}$$

$$s \ge 0, \qquad \qquad s \le M_2 y, \tag{B.1}$$

where M_1, M_2 are interval bounds. Constraints (B.1) are added layer-wise with pyscipopt-ml.add_predictor_constr. We keep SCIP 8.0.4 at default settings.

- c) Pros & Cons.: The formulation is exact but may inject thousands of binaries, making solve time explode for deep nets; nonetheless it provides a strong, certifiable reference point.
 - 2) Single-Step Gradient (SSG) Heuristic:
- a) Rationale.: SSG drops integrality during optimisation: discrete variables are relaxed to their continuous domain, smooth penalties enforce the original constraints, and first-order updates run entirely in PyTorch. A final rounding step returns a feasible integer solution.
- b) Workflow.: Algorithm 2 summarises the procedure. The relaxed vector \boldsymbol{x} is initialised inside its box bounds; in each iteration we back-propagate through the network, take an Adam step on the penalised objective, and project back to the box. Whenever a fully feasible iterate is encountered we record its objective value; the best one is returned after T iterations. The method involves no external solver, so its cost is dominated by forward/backward passes.
- c) Hyper-parameters.: We fix T=100, learning-rate schedule $\eta_t=10^{-2}\cdot(1+0.01t)^{-0.5}$, and penalty weights $\mu_{\rm lin}=\mu_{\rm nn}=50$ in all experiments; a brief grid search on a held-out validation set produced these values.
- d) Pros & Cons.: SSG is light-weight and highly parallelisable but provides no optimality certificate and may return sub-optimal solutions if the penalty weights are not well tuned.

B. Datasets

1) Water Potability Benchmark: This benchmark corresponds to the WP problem type in SURROGATELIB[14]—a library of mixed-integer programs that embed machine-learning predictors as surrogate constraints. This benchmark portrays the work of a public–health agency that must transform a collection of unsafe water samples into drinkable ones while operating under strict treatment budgets. Each raw sample is described by a nine–dimensional feature vector $w_i \in \mathbb{R}^9, i \in [n]$, where [n] denotes the index set of the initially non-potable samples.

Algorithm 2 Single-Step Gradient (SSG) Heuristic

Require: initial x^0 , bounds $\underline{x}, \overline{x}$, steps $\{\eta_t\}_{t=1}^T$, penalties $\mu_{\text{lin}}, \mu_{\text{nn}}$

```
Ensure: best feasible pair (\hat{x}, \hat{O})

1: \hat{O} \leftarrow +\infty, \hat{x} \leftarrow \varnothing

2: for t = 1, ..., T do

3: Forward: compute p_{\text{lin}} = \max\{0, A_{\text{MIP}}x^{t-1} - b_{\text{MIP}}\}, p_{\text{nn}} = \max\{0, A_{\text{NN}}[x^{t-1}; f_{\theta}(x^{t-1})] - b_{\text{NN}}\}

4: \mathcal{L} \leftarrow c^{\top}x^{t-1} + d^{\top}f_{\theta}(x^{t-1}) + \mu_{\text{lin}}\|p_{\text{lin}}\|_{2}^{2} + \mu_{\text{nn}}\|p_{\text{nn}}\|_{2}^{2}

5: Backward: x^{t} \leftarrow \text{Proj}_{[\underline{x},\overline{x}]}(x^{t-1} - \eta_{t}\nabla_{x}\mathcal{L})

6: if p_{\text{lin}} = p_{\text{nn}} = 0 and c^{\top}x^{t} < \hat{O} then

7: \hat{O} \leftarrow c^{\top}x^{t}, \hat{x} \leftarrow \text{round}(x^{t})

8: end if

9: end for

10: return (\hat{x}, \hat{O})
```

- a) Decision variables.: For every sample i and attribute j we introduce
 - $a_{i,j} \ge 0$: upward adjustment applied to attribute j,
 - $b_{i,j} \ge 0$: downward adjustment applied to attribute j,
 - $x_{i,j}$: value of attribute j after treatment,
 - $y_i \in \{0,1\}$: indicator that equals 1 if sample i is potable post-treatment.
- b) Budgets.: Each attribute $j \in [9]$ has independent non-negative budgets γ_j^+, γ_j^- limiting the total upward (a) and downward (b) changes across all samples.
- c) Potability oracle.: A pre-trained classifier $f: \mathbb{R}^9 \to \{0,1\}$ returns 1 when its input vector is judged drinkable.
- d) Mixed-integer formulation.: The optimisation problem is

$$\max_{a,b,x,y} \quad \sum_{i=1}^{n} y_{i}$$
s.t.
$$x_{i,j} = w_{i,j} + a_{i,j} - b_{i,j} \qquad \forall i \in [n], j \in [9],$$

$$\sum_{i=1}^{n} a_{i,j} \leq \gamma_{j}^{+} \qquad \forall j \in [9],$$

$$\sum_{i=1}^{n} b_{i,j} \leq \gamma_{j}^{-} \qquad \forall j \in [9],$$

$$y_{i} = f(x_{i}) \qquad \forall i \in [n],$$

$$a_{i,j}, b_{i,j} \geq 0, \quad y_{i} \in \{0, 1\}.$$
(16)

The objective maximises the count of samples deemed potable while ensuring that the cumulative treatment applied to each attribute stays within the allotted budgets. Data for this problem is publicly available².

2) Tree Planting Benchmark: This benchmark (TP in SUR-ROGATELIB [14]) models the work of a forestry agency that must re-plant a cleared strip of land. The agency wishes to maximise the total expected number of trees that survive while (i) respecting a limited budget for soil sterilisation and planting

²https://github.com/MainakRepositor/Datasets/tree/master

costs and (ii) guaranteeing a minimum expected survival target for every tree species considered.

- a) Instance data.: A grid of n candidate planting locations is generated; each location $i \in [n]$ is described by a seven-dimensional feature vector $x_i \in \mathbb{R}^7$ that includes soil, light and moisture indicators as well as a sterilised flag (initially 0). Four tree species are available, indexed by $k \in [4]$. For every species k we are given a minimum expected survival requirement $\gamma_k \in \mathbb{R}_{\geq 0}$, a planting cost $c_k \in \mathbb{R}_{\geq 0}$, and a trained surrogate predictor $f_k : \mathbb{R}^7 \to [0,1]$ returning the probability that species k survives at a given location.
- b) Decision variables.: For each location i and species k:
 - $p_{i,k} \in \{0,1\}$: 1 iff species k is planted at location i;
 - $s_{i,k} \in [0,1]$: predicted survival probability of k at i (output of the surrogate);
 - $s'_{i,k} \in [0,1]$: survival contribution that is counted in the objective;

and for every location $z_i \in \{0,1\}$ indicates whether its soil is sterilised.

- c) Budgets and targets.:
- Sterilisation budget $\beta \in \mathbb{N}$ limits the number of sites that can be sterilised.
- Planting budget $B \in \mathbb{R}_{\geq 0}$ bounds the total cost of saplings.
- Species-wise targets γ_k ensure biodiversity.
 - d) Mixed-integer formulation .:

C. Convergence Proof for Theorem V.1

We reproduce the augmented-Lagrangian merit

$$\mathcal{M}_{\rho}(x,u,\lambda) := g(u) + c^{\top}x + \frac{\rho}{2} \left\| u - x + \frac{\lambda}{\rho} \right\|_2^2 - \frac{1}{2\rho} \|\lambda\|_2^2,$$

where $g(u) = d^{T} f_{\theta}(u)$. Under Assumption 1 the following properties hold.

Lemma A.1 (Strong convexity of the u-block). For $\rho > L$ the map $u \mapsto g(u) + \frac{\rho}{2} \|u - x\|_2^2$ is $(\rho - L)$ -strongly convex and $(\rho + L)$ -smooth.

Proof. g is L-smooth and convex; adding $\frac{\rho}{2}\|u-x\|_2^2$ increases both curvature bounds by ρ . \square

Lemma A.2 (Per-iteration decrease). Let $(x^{(k)}, u^{(k)}, \lambda^{(k)})$ be the k-th iterate. Then

$$\mathcal{M}_{\rho}^{(k+1)} \leq \mathcal{M}_{\rho}^{(k)} - \frac{\rho - L}{2} \|u^{(k)} - x^{(k)}\|_{2}^{2}.$$

Proof. (i) u-update. By Lemma A.1 and exact minimisation, $\mathcal{M}_{\rho}(x^{(k-1)}, u^{(k)}, \lambda^{(k-1)}) \leq \mathcal{M}_{\rho}(x^{(k-1)}, u^{(k-1)}, \lambda^{(k-1)}) - \frac{\rho-L}{2} \|u^{(k)} - u^{(k-1)}\|_2^2.$

(ii) x-update. Since \mathcal{X} is finite and the MIP subproblem is solved optimally, $\mathcal{M}_{\rho}(x^{(k)}, u^{(k)}, \lambda^{(k-1)}) \leq \mathcal{M}_{\rho}(x^{(k-1)}, u^{(k)}, \lambda^{(k-1)})$.

(iii) Dual update. Setting $\lambda^{(k)} = \lambda^{(k-1)} + \rho(u^{(k)} - x^{(k)})$ gives $\mathcal{M}_{\rho}(x^{(k)}, u^{(k)}, \lambda^{(k)}) = \mathcal{M}_{\rho}(x^{(k)}, u^{(k)}, \lambda^{(k-1)}) - \frac{\rho}{2} \|u^{(k)} - x^{(k)}\|_2^2$. Combining (i)–(iii) and using $\|u^{(k)} - u^{(k-1)}\|_2 \le \|u^{(k)} - x^{(k)}\|_2 + \|x^{(k)} - u^{(k-1)}\|_2$ yields the claimed inequality.

a) Proof of Theorem V.1.: Summing Lemma A.2 over k and noting that \mathcal{M}_{ρ} is bounded below (by $-\|\lambda\|_2^2/(2\rho)$) proves $\sum_k \|u^{(k)} - x^{(k)}\|_2^2 < \infty$ and thus (13). Boundedness follows from the coercivity of \mathcal{M}_{ρ} in (x,u) and the finite cardinality of \mathcal{X} . A convergent subsequence exists by Bolzano–Weierstrass; continuity of $\nabla_u \mathcal{L}_{\rho}$ and exact optimality of both subproblems imply that every limit point satisfies the KKT conditions (12).

D. Proof of Linear Scalability (Theorem V.2)

We detail the cost of one outer iteration.

- a) MIP step.: The discrete block (9) contains p integer variables and m_1 linear constraints, independent of the NN width or depth. Let $T_{\rm MIP}$ denote the time needed by the branch-and-bound solver; this is treated as an oracle cost.
- b) NN step.: Evaluating $f_{\theta}(u)$ requires one forward pass through the network; computing a vector–Jacobian product for g needs one reverse pass. For dense or convolutional layers both passes are $\Theta(P)$ flops [33]. The projection (PGD) or the Newton barrier uses only the m_2 affine rows of $A_{\rm NN}$, whose dimension is fixed by the application, hence O(1) w.r.t. P.
- c) Total.: Adding the two independent costs yields $T_{\text{iter}} = \Theta(T_{\text{MIP}} + P)$, proving Theorem V.2.